Original Article
J. Korean Wood Sci. Technol. 2022, 50(5): 353-364
https://doi.org/10.5658/WOOD.2022.50.5.353

Journal of the Korean Wood Science and Technology
pISSN: 1017-0715 eISSN: 2233-7180
http://www.woodj.org

Synchrotron X-Ray Diffraction Studies on Crystalline Domains in Urea–Formaldehyde Resins at Low Molar Ratio

Eko Setio WIBOWO[1] · Byung-Dae PARK[1,†] · Valerio CAUSIN[2] · Dongyup HAHN[3,4]

ABSTRACT

The crystalline domain of thermosetting urea–formaldehyde (UF) resins at low formaldehyde-to-urea (F/U) molar ratios (≤ 1.0) is known to be responsible for their poor performance as wood adhesives. Crystallization has been observed in 1.0 F/U UF resins during the addition reaction stage and at the end of the synthesis process (neat UF resins). The crystallinity and X-ray diffraction (XRD) spectra of the uncured neat UF resins, on the other hand, differed significantly from those of the cured neat UF resins, raising the possibility that their crystal structures were also different. This study demonstrates for the first time that the crystalline domains in 1.0 F/U UF resins generated from uncured and cured samples are identical. Despite having a lower crystallinity value, the synchrotron XRD patterns of purified neat UF resins were equivalent to the XRD patterns of cured neat UF resins. Transmission electron microscope images of the cured UF resins showed that the crystals were lamellar structures. This finding suggests that the crystal at low molar ratio UF resins are isotropic polycrystals with random orientation.

Keywords: urea–formaldehyde resins, wood adhesives, crystalline polymer, synchrotron X-ray diffraction, hydrogen bonding

1. INTRODUCTION

Urea–formaldehyde (UF) resins are the most widely used adhesives in the wood-based products industry. They have long been recognized as a constituent of thermosetting polymers, which typically have an amorphous structure. For several years, various research on the use of amino resins for wood-based panels have been conducted by many researchers (Han *et al*., 2019; Hong *et al*., 2017; Jeong and Park, 2019; Jeong *et al*., 2020; Kim and Park, 2021a; Kim and Park, 2021b; Lubis *et al*., 2019a, 2019b; Wibowo *et al*., 2021). Surprisingly, researchers have uncovered a unique property of UF resins: the formation of crystalline domains (Despres and Pizzi, 2006; Levendis *et al*., 1992; Li and Zhang, 2021; Liu *et al*., 2017; Nuryawan *et al*., 2017; Park and Causin, 2013; Park and Jeong, 2011; Pratt *et al*., 1985; Singh *et al*., 2014; Stuligross and Koutsky, 1985).

Date Received July 4, 2022, Date Revised July 28, 2022, Date Accepted September 8, 2022
[1] Department of Wood and Paper Science, Kyungpook National University, Daegu 41566, Korea
[2] Dipartimento di Scienze Chimiche, Universita di Padova, Padova 35131, Italy
[3] School of Food Science and Biotechnology, Kyungpook National University, Daegu 41566, Korea
[4] Department of Integrative Biology, Kyungpook National University, Daegu 41566, Korea
[†] Corresponding author: Byung-Dae PARK (e-mail: byungdae@knu.ac.kr, https://orcid.org/0000-0002-9802-7855)

Apparently, the attempt of lowering the formaldehyde-to-urea (F/U) molar ratio (≤1.0) in UF resins to achieve low formaldehyde emission (Lubis and Park, 2020; Myers, 1984; Pizzi *et al.*, 1994) of wood-based panels causes the formation of crystalline domains (Park and Causin, 2013; Park and Park, 2021). The generation of crystalline domains in low molar ratio UF resins unfortunately can reduce cohesion by blocking three-dimensional cross-linking, resulting in poor adhesion to wood-based products (Levendis *et al.*, 1992; Wibowo *et al.*, 2020a). Furthermore, it was discovered that these crystalline domains were built with a lamellar structure surrounded by amorphous layers, classifying them as semicrystalline (Wibowo and Park, 2021). Interestingly, our recent work demonstrated that UF resins with a low molar ratio crystallize when cured in contact with wood (Singh *et al.*, 2014), which contradicted earlier beliefs that crystalline domains in UF resins could not be observed when cured in contact with wood in the covered glue line (Levendis *et al.*, 1992). Another fascinating observation was the presence of crystalline domains of UF resins in liquid form (Nuryawan *et al.*, 2017). Transmission electron microscopy (TEM) was used in their study to examine the morphologies of liquid UF resins with two distinct F/U molar ratios (1.6 and 1.0). These findings confirmed the presence of crystalline structures in UF resins with low F/U molar ratios, even in form of liquid, implying that the crystal is present even before curing.

Thus, in a recent work, we attempted to clarify crystallization in liquid UF resins and identify the phenomena that cause crystallization during the synthesis (Wibowo *et al.*, 2020b). In this study, several samples from different stages of the synthesis of low molar ratio UF resins were isolated to find out where crystallization happened. The results revealed that crystal domains developed in low molar ratio UF resins during the addition reaction (#1) and after the addition of urea at the end of the synthesis step (#2) (Fig. 1). Further, it was concluded that the addition of secondary urea at the end of

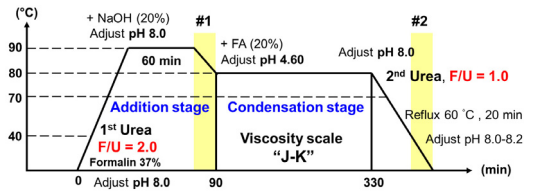

Fig. 1. Schematic diagram of the synthesis steps of UF resin and the crystallization region (stages #1 and #2) occurred. Copyright 2022. Modified with permission from ACS Publications (Wibowo and Park, 2022).

synthesis stage of UF resins split a large proportion of various branched linkages, which were formed earlier in the synthesis of the resins at the condensation stage, resulting in linear molecules that have an ordered structure preserved by hydrogen bonding. Thus, it was confirmed that linear molecules, as well as hydrogen bonding between them, were responsible for the crystallization of UF resins (Wibowo and Park, 2022).

However, the X-ray diffraction (XRD) pattern shape of the 1.0 F/U UF resins derived from cured and uncured samples significantly differs, suggesting that their crystal structures may be different. For example, in the XRD spectra of cured UF resins, there are four primary crystalline peaks (Liu *et al.*, 2017; Park and Jeong, 2011; Wibowo and Park, 2021), but an uncured sample has one main sharp peak and multiple smaller sharp peaks (Wibowo *et al.*, 2020b). Therefore, whether the crystals that exist in these different conditions are the same crystal is still unclear. In this work, we attempt to identify the actual crystalline species of UF resins by isolating and purifying the crystal samples from stages #1 and #2. For this purpose, dialysis method was used, and the purified samples were analyzed with synchrotron XRD. Dialysis is a commonly used method in macromolecular chemistry to purify polymers and polymerization solutions by removing undesirable impurities, including unreacted monomers and other small substances (Schuett *et al.*, 2021). Small impurities with a specified hydrody-

namic radius flow through a membrane because of diffusion, whereas larger macromolecules are retained by the dialysis membrane. In this case, unreacted urea and small crystals consisting of small oligomers such as mono and di(hydroxymethyl) urea can be eliminated from UF resins. The purified UF resins crystal can be characterized by X-ray crystallography. However, to obtain high-resolution XRD spectra, a more sophisticated XRD technique is required. In recent years, an advanced technique for acquiring high-resolution and accurate XRD spectra, such as synchrotron XRD, has been developed (Baruchel *et al.*, 2013; Lin *et al*., 2017; Sedigh Rahimabadi *et al*., 2020). Synchrotron radiation is based on the physical phenomenon (classical electrodynamics) in which a moving charged particle (electron) generates energy as it changes direction at a relativistic speed (Lin *et al*., 2017). When electron beams are accelerated (bent) by magnetic fields, electromagnetic radiation is produced. The electromagnetic radiation emitted through bending magnets spans a wide range of wavelengths from infrared to hard X-ray (Sedigh Rahimabadi *et al*., 2020). The released energy is at an X-ray wavelength when an electron travels fast enough. The resulting X-rays are emitted in dozens of narrow beams; each focused on a beamline near to the accelerator. Synchrotron radiation facilities generate high-flux, monochromatic, highly collimated X-ray beams with great brightness compared to conventional laboratory XRD (Sedigh Rahimabadi *et al*., 2020). Moreover, the energy of the radiated beams can be adjusted in such a way that excellent signal-to-noise ratio signals are obtained. As a result of the advantages of synchrotron X-ray, the detailed studies of crystalline, amorphous, and complex structures are feasible. This technique may be used to investigate various systems, including powders, thin films, and bulk forms with complicated crystalline or amorphous structures. Because of these advantages, synchrotron XRD is employed to examine the actual crystalline species of purified UF resins. Moreover, TEM is used to observe the morphology of crystalline domains in UF resins and compare it to the results of synchrotron XRD.

2. MATERIALS and METHODS

2.1. Materials

Formalin (37 wt%) and extra pure grade urea (99 wt%) were obtained from Daejung Chemical, Korea. Extra pure grade NH_4Cl (99 wt%), NaOH (93 wt%), and aqueous formic acid (85 wt%) were purchased from Duksan Chemical, Korea. The SnakeSkin® pleated dialysis tubing, 7000 MWCO, was purchased from Thermo Scientific (Waltham, MA, USA).

2.2. Synthesis and purification of low molar ratio urea-formaldehyde (UF) resins

UF resins with F/U molar ratio of 1.0 was synthesized via an established alkaline－acid－alkaline three-step reaction. Fig. 1 summarizes the UF resins synthesis procedure. In brief, formalin solution was placed into a four-neck glass reactor, pH was adjusted to 8.0 using NaOH (20 wt%), and the temperature was raised to 40℃. Urea was then added to the reactor, yielding in an initial F/U molar ratio of 2.0. To allow the addition process to occur, the liquid was heated to 90℃ and the pH was maintained at 8.0 for 1 h. Subsequently, the temperature and pH were adjusted to 80℃ and 4.6, respectively, to promote the condensation reaction. When a target viscosity of 'J-K' scale was obtained based on readings using a standard bubble viscometer (VG 900, Gardener-Holdt, Columbia, SC, USA), the reaction was terminated, and the pH was adjusted back to alkaline (8.0-8.2). A certain amount of urea was also added to the glass reactor to reach a final F/U molar ratio of 1.0, and the temperature was maintained at 60℃ for 20 minutes. The resins were then cooled to 25℃ and the

pH was adjusted to 8.2. Prior to analysis, the resins were stored at room temperature for 24 h. Fig. 1 shows the position where the liquid resin has been sampled and labeled as samples #1 and #2. Sample #1 was taken at the end of the addition stage and the sample #2 was taken at the final stage after adjusting the pH to 8.0–8.2.

2.3. Synchrotron X-ray diffraction of urea–formaldehyde (UF) resins

Prior to synchrotron XRD analysis, sample #1 and #2 were dried in an oven at 50℃ and crushed to a fine powder. Afterwards, the powdered sample was purified using a dialysis process. Approximately, 50–100 mg of each sample was put in the SnakeSkin pleated dialysis tubing, which was filled with roughly 40–50 mL distilled water. The tubes were sealed on both sides and submerged in 1,000 mL of distilled water. The dialysis was performed for 7 days, after which the residue was dried to provide a pure sample. Furthermore, synchrotron XRD data were collected at the 7A beamline of the Pohang Accelerator Laboratory (PAL, Pohang, Korea), Pohang Light Source II (wavelength of 0.9793 Å, beam size of 100 μm), under nitrogen cold stream (100 K). Data were collected using the oscillation method in intervals of 1° step on an ADSC Quantum 270 CCD detector (Area Detector Systems, Poway, CA, USA) with a crystal-to-detector distance of 120 mm (Kim *et al*., 2020). As a comparison, unpurified sample #1, unpurified sample #2, and cured sample #2 (prepared by adding 3% NH_4Cl and put in an oven at 120℃ for 1 h) were characterized using laboratory XRD (D/Max-2500, Miniflex II, Rigaku, Tokyo, Japan) with a Cu Kα radiation source (λ = 0.15406 nm). The samples were scanned at room temperature from 0 to 50° with a step of 0.02°/min. Furthermore, the crystallinity values of UF resins were determined from XRD patterns using the peak deconvolution method using a Gaussian function (Wibowo and Park, 2020). The crystallinity of each sample was calculated as follows:

$$Crystallinity\ (\%) = \frac{S_c}{S_c + S_a} \times 100 \quad (1)$$

where, S_c and S_a represent the area of the crystalline domain and the area of amorphous domain, respectively.

2.4. Transmission electron microscopy

TEM investigation was performed according to the published method to observe the morphology of crystalline domains in UF resins (Singh *et al*., 2015). To prepare the sample for TEM investigation, a small piece of radiata pine (*Pinus radiata* D. Don) veneer with dimensions of 25 mm × 35 mm × 6 mm was impregnated in a glass beaker filled with cured neat UF resins containing 0.1% NH_4Cl as hardener. Furthermore, the sample was placed in a vacuum drier for impregnation at ambient temperature under a pressure of 67.7 kPa for 24 h. Then, the sample was pre-cured in a vacuum drier for 24 h at 60℃ and 67.7 kPa. The ultrathin sections were obtained using an ultramicrotome and a diamond knife. The slices were stained for 7 min with a 2% aqueous uranyl acetate solution before being examined with an H-7100 Hitachi TEM at 75 kV and a detector X Max.

3. RESULTS and DISCUSSION

3.1. Crystalline domains of urea–formaldehyde (UF) resins

The formation of crystal domains in UF resins with low molar ratios has been extensively studied, and it has been revealed that such crystal formation decreases the adhesive strength of UF resins while compensating for decreased formaldehyde emission (Despres and Pizzi, 2006; Keith Dunker *et al*., 1986; Park *et al*., 2011; Pratt *et al*., 1985; Stuligross and Koutsky, 1985). Their adhesive strength deteriorates due to a decrease in cohesive force caused by the restriction of crosslinking formation.

In fact, the molecules organized in the crystal lattice cannot contribute in the construction of the UF resin crosslinked structure, but are instead held together by relatively weak intermolecular interactions (Ferg *et al*., 1993). The cured samples of thermosetting polymers typically have a strong three-dimensional network or cross-linking that is covalently bonded that holds the polymer chains together. Thus, any crystalline domain in the polymer structure may obstruct the establishment of a three-dimensional cross-linking network (Wibowo *et al*., 2022). Moreover, in low molar ratio UF resins, crystalline domains are constructed by linear structures that are held together by hydrogen bonding (Wibowo and Park, 2021), which is not as strong as covalent bonding and hence leads to a weak cohesive force. It is expected that by understanding the definite crystalline structure of UF resins, it would be possible to simply modify the structure of UF resins to prevent the degradation of their cohesive force. Fig. 2 depicts a comparison of UF resins isolated at different stages of synthesis and treated under various conditions. Fig. 2(a) and (b), for example, compare unpurified samples of #1 and #2. There are clear differences, primarily in the shape of the spectra and the number of the peaks, in sample #1, several peaks represent the crystalline domains are possibly belong to the crystal structures of unreacted urea or small crystals composed of mono-, bis-, and tris(hydroxymethyl) urea (Park and Jeong, 2011; Wibowo *et al*., 2020b). This is due to the fact that, as previously reported (Wibowo *et al*., 2020b), the crystalline peaks of UF model compounds (mono-, bis-, and tris(hydroxymethyl) urea) matched with the crystalline peaks of sample #1. In contrast, the spectrum of sample #2 shows a clear combination of crystalline and amorphous characteristics, as indicated by the sharp crystalline peak with multiple minor peaks and a noticeable amorphous underneath it. This is an indication of a semicrystalline nature. Another significant difference could be seen in their crystallinities and crystallite sizes. It has been reported that the crystallinity of sample #1 differed from that of sample #2, which is around 57% and 42% for sample #1 and #2, respectively (Wibowo *et al*., 2020b). In addition, in the XRD patterns of samples #1 and #2, the average crystallite sizes associated with the crystalline peaks were around 6.5 nm and 34.4 nm, respectively (Wibowo *et al*., 2020b). These findings revealed that the crystallite size in sample #1 was smaller than that in sample #2, implying that the crystalline domains of sample #2 may be made up of longer and more regular polymers than those of sample #1. Furthermore, Fig. 2(c) and (d) display the synchrotron XRD spectra of samples #1 and #2 following dialysis purification. The XRD spectra before [Fig. 2(a) and (b)] and after purification clearly show a significant transformation [Fig. 2(c) and (d)]. For example, the intensity of several crystalline peaks in sample #1 [Fig. 2(c)] decreased dramatically, suggesting that certain crystal components were eliminated. Interestingly, the second peak from the left was the most decreased peak in the XRD spectra; this peak might be attributable to unreacted urea or mono(hydroxymethyl) urea crystals. This is because the XRD pattern in Fig. 2(a) was most likely a combination of mono-, bis-, and tris(hydroxymethyl) urea XRD patterns, whereas the XRD pattern in Fig. 2(c) was very similar to the XRD pattern of the bis(hydroxymethyl) urea model compound (Park and Jeong, 2011; Wibowo *et al*., 2020b), indicating that the majority of the bis(hydroxymethyl) urea crystal was preserved. As illustrated in Fig. 3(a), the crystalline structure of bis(hydroxymethyl) urea might be stronger than that of mono(hydroxymethyl) urea due to the greater number of hydrogen bonds that can be formed. As a result, mono(hydroxymethyl) urea was easy to separate from the primary structure, dissolve in water, and pass through the dialysis membrane [Fig. 3(b)]. Surprisingly, the most striking XRD pattern alteration was discovered in Fig. 2(d). After purification, sample #2 was completely different from the unpurified one; the pattern was more similar to the cured sample #2

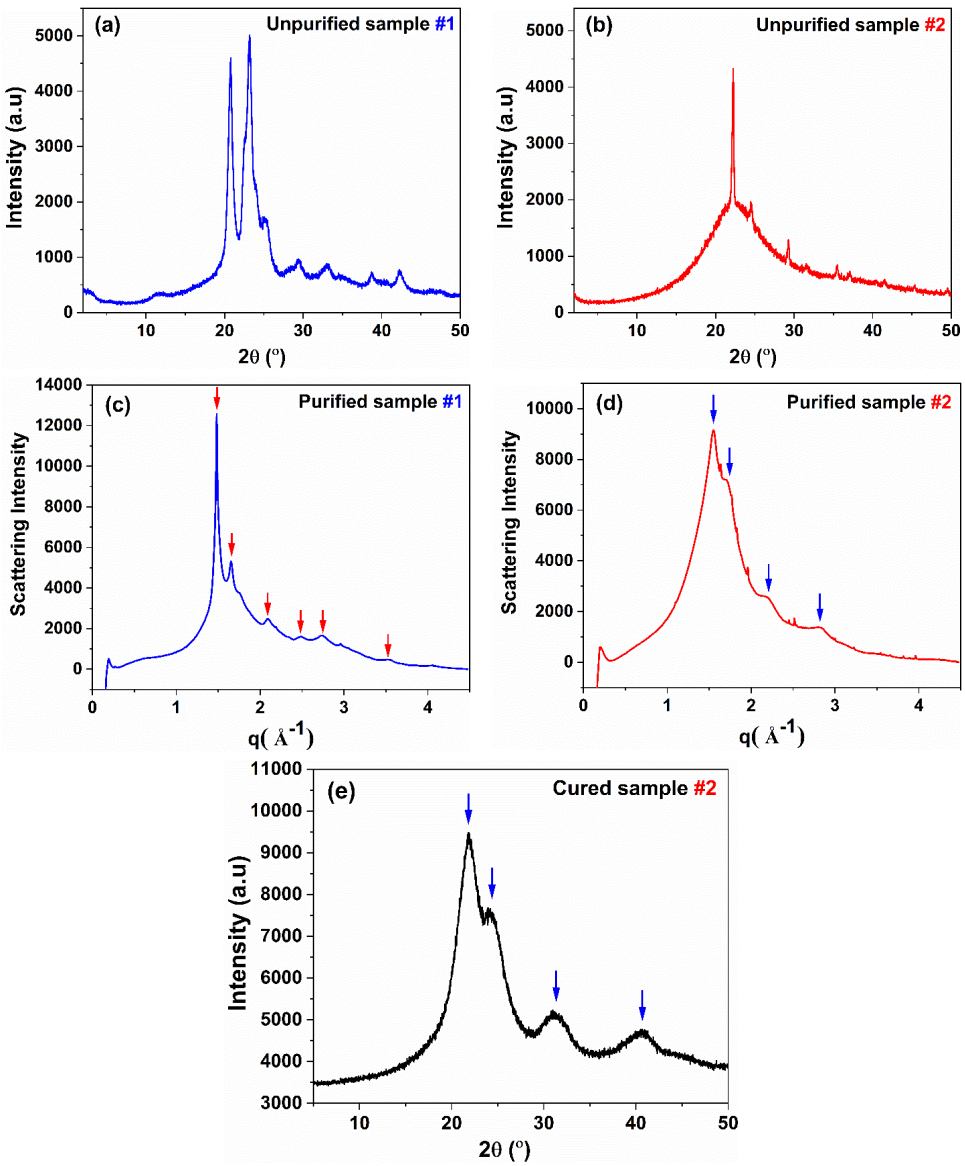

Fig. 2. X-ray diffraction spectra of 1.0 F/U UF resins isolated at different stages of synthesis and treated under various conditions: (a) unpurified sample #1, (b) unpurified sample #2, (c) purified sample #1, (d) purified sample #1, and (e) cured sample #2. UF: urea–formaldehyde.

depicted in Fig. 2(e). During dialysis, it seems that most of the crystals and some amorphous parts of unpurified sample #2 were eliminated, leaving the original crystalline domain of UF resins as illustrated in Fig. 3(b). The removed crystals were primarily composed of unreacted urea and small crystal domains assigned to mono(hydroxymethyl) urea and short linear oligomers. Meanwhile, the amorphous components that were liberated were

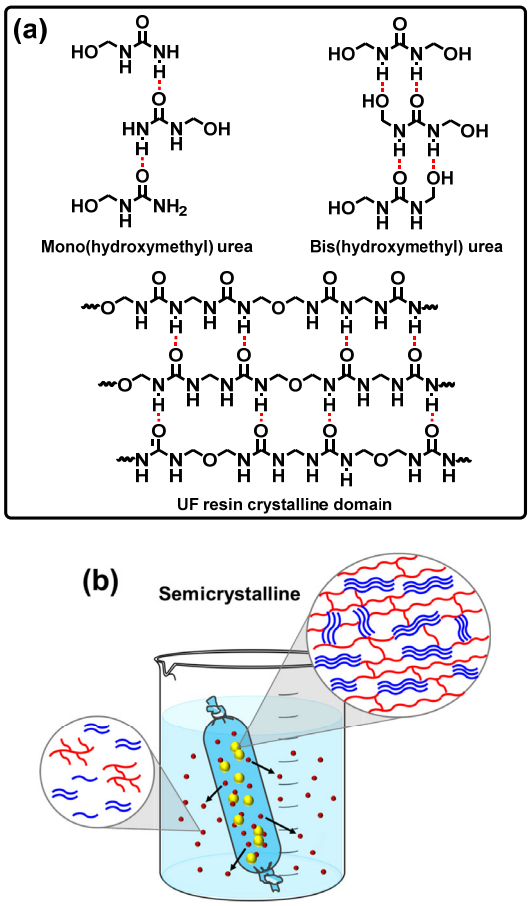

Fig. 3. Schematic representations of (a) chemical structures of possible crystalline domains in UF resins and (b) the dialysis process and crystal structure visualization of UF resins. UF: urea–formaldehyde.

attributable to the oxymethylene formaldehyde and short methylene ether linkages that formed during synthesis (Steinhof *et al*., 2014; Wang *et al*., 2018; Wibowo *et al*., 2020b). The fact that the XRD patterns in Fig. 2(d) and (e) were so identical suggested that the original crystalline domain of UF resins was present even before curing. The curing process simply improves the development of crystalline domains by using an acid catalyst. The hardener appears to promote linear structural elongation, hence enhancing hydrogen bonding formation and resulting in a more pronounced crystal structure and sharper XRD pattern. This is supported by prior study, which shown that the crystallinity value of cured UF resins rose as the percentage of hardener increased (Wibowo and Park, 2020). The typical crystalline domain of UF resins, as aforementioned, was constituted of linear oligomers stacked together by hydrogen bonding force [Fig. 3(a)]. This type of structure was strong enough to be maintained in the primary structure of the solid sample because of the high number of hydrogen bonds, as well as because these crystalline domains were covalently bonded to the surrounding amorphous structure of UF resins (Wibowo and Park, 2021). Thus, even after dialysis, the crystalline domain remains in sample #2, as demonstrated in [Fig. 3(b)].

Interestingly, the crystallinity of purified samples #1 and #2 calculated from the deconvoluted XRD spectra of Fig. 4 reduced to 52% and 40%, respectively, when compared to the unpurified ones, corroborating the hypothesis that some crystals were removed during dialysis. Further, the crystallinity of purified sample #2 is 40%, which is lower than that of cured sample #2 [i.e., 52% (Wibowo and Park, 2021; Wibowo *et al*., 2020a)]. This finding indicates that, although the purified sample #2 contains the original crystalline domain of UF resins, its crystallinity is smaller than that of cured sample #2. Additionally, based on the similarities in XRD pattern, it is possible to assume that their crystal structure is the same [Fig. 3(b)]. Furthermore, Fig. 5 depicts the two-dimensional (2D) diffractogram of UF resins isolated at different stages of synthesis. The 0° angle denotes parallel radiation of the incident X-ray beam to the sample, whereas the 90° angle denotes perpendicular radiation of the incident X-ray beam to the sample. Fig. 5(a) demonstrates that sample #1 has a greater number of concentric circles (Debye rings). Meanwhile, sample #2 has less concentrated rings, which are roughly four circles at most [Fig. 5(b)]. This suggests that sample #2 comprised fewer crystalline domains than sample #1, as evi-

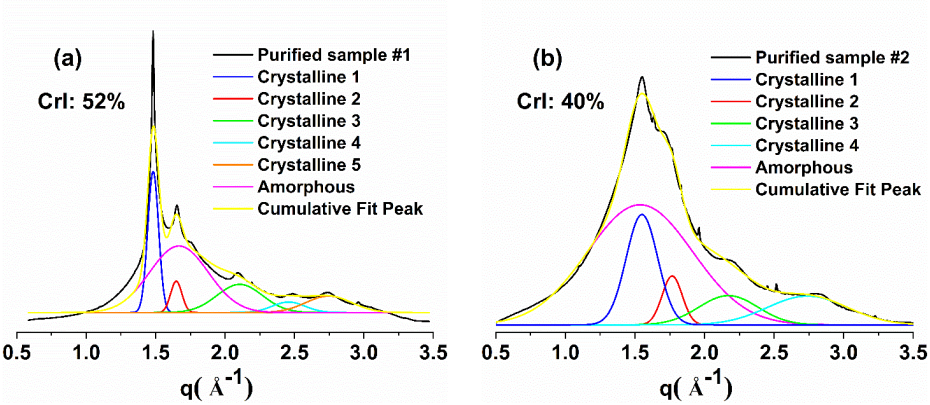

Fig. 4. Deconvoluted synchrotron X-ray diffraction spectra of purified UF resins isolated at different stages of synthesis: (a) sample #1, (b) sample #2. UF: urea–formaldehyde.

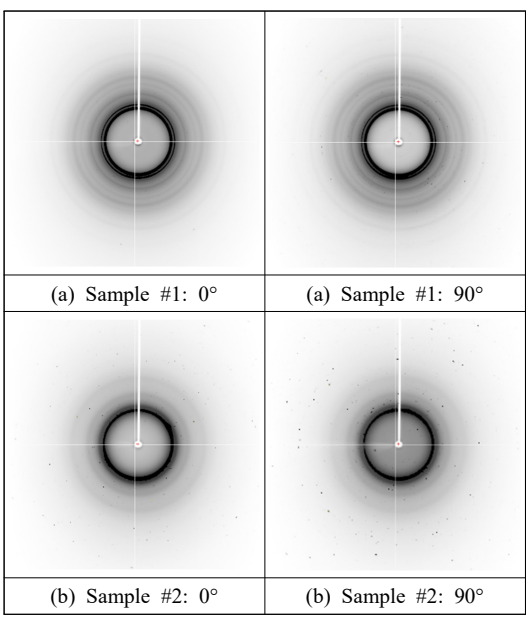

Fig. 5. Two-dimensional synchrotron X-ray diffraction pattern of purified UF resins isolated at different stages of synthesis (a) sample #1, (b) sample #2. UF: urea–formaldehyde.

denced by the lower number of crystalline peaks in the XRD spectra and degree of crystallinity. A radial slice of a 2D diffractogram is known to offer the traditional XRD pattern of intensity vs. $\vec{q}$. The angular slice of the 2D diffractogram, on the other hand, offers information on the texture of the sample. For example, a perfect polycrystalline sample exhibits full Debye rings, whereas single crystals show as dots, and an amorphous material has no distinctive features (Widjonarko, 2016). In the case of UF resins, the 2D diffractograms of samples #1 and #2 exhibit perfect circles, indicating that the crystals in the sample are isotropic polycrystals with no preferred (random) orientation relative to the incident electron beam (Singh *et al.*, 2014). The crystalline domains of UF resin with no specified orientation was illustrated in Fig. 3(b).

The morphology of cured neat UF resins (sample #2) was observed using TEM (Fig. 6). The resins were impregnated in a wood veneer to visualize the morphology of resins present in the lumen of tracheid. Fig. 6 shows a high-resolution TEM image with a magnification of 400k. Remarkably, several lamellar structures representing a cluster of individual polymer chain were observed at some specified sites (e.g., yellow circle), whereas other areas comprised of irregular amorphous structures. The well-ordered lamellae were formed as a result of hydrogen bonding between the C = O and N−H groups

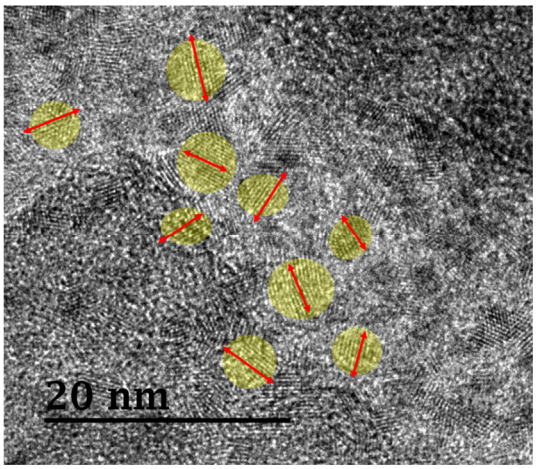

Fig. 6. A TEM image of cured neat UF resins (sample #2) demonstrating the random orientation of crytsallin domains. TEM: transmission electron microscopy, UF: urea–formaldehyde.

of linear oligomers of UF resins as previously reported in literature (Wibowo and Park, 2021, 2022). Moreover, these lamellar crystalline domains clearly have a random orientation (as indicated by the red arrow), which is consistent with the 2D synchrotron XRD pattern that shows full Debye rings (Fig. 5). Furthermore, the TEM image (Fig. 6) shows that UF resins have a typical semicrystalline morphology, with a random orientation of crystal lamellae domains surrounded by amorphous regions, as previously illustrated by the Fig. 3(b). Surprisingly, the lamellae of cured UF resins are similar to those found in polypeptide crystals. A recent study used TEM to demonstrate an individual chain of the particular protein-like polymers (Drnovšek *et al*., 2016). They discovered polypeptide lamellae coupled with a β-sheet structure, which is comparable to what was discovered in this study. Moreover, TEM images of different types of semicrystalline polymers reported by many research published in the literature were remarkably similar to our findings (Kuei *et al*., 2020; Libera and Egerton, 2010; Tosaka *et al*., 2005).

4. CONCLUSIONS

In the current study, the crystalline domains of UF resins were identified by isolating and purifying crystal samples collected at the end of the addition stage (sample #1) and at the end of the synthesis process (sample #2). The samples were purified by dialysis and then analyzed using synchrotron X-ray diffraction. The results revealed that the crystal structures of sample #1 may be constituted of unreacted urea or small crystals comprised of mono-, bis-, and tris(hydroxymethyl) urea. Sample #2, on the other hand, has a clear combination of crystalline and amorphous characteristics. The XRD pattern of purified sample #2 is identical to that of cured sample #2, indicating that their crystal type is the same, which is a semicrystalline crystal. This crystalline domain of neat UF resins (sample #2) was most likely composed of linear oligomers packed together by hydrogen bonding and covalently connected to the surrounding amorphous structure. Furthermore, 2D diffractograms of both samples exhibit a polycrystalline feature with no preferential orientation relative to the incident electron beam. This is further supported by the TEM image of cured sample #2, which demonstrates that the lamellar crystalline domain exhibited a random orientation. In addition, it is concluded that the type of crystal discovered in purified sample #2 is the origin or actual crystalline domain of low molar ratio UF resins.

CONFLICT of INTEREST

No potential conflict of interest relevant to this article was reported.

ACKNOWLEDGMENT

This work was supported by the National Research Foundation (NRF) of Korea funded by the Korean Government (MSIT) (Grant No. 2020R1A2C1005042).

REFERENCES

Baruchel, J., Di Michiel, M., Lafford, T., Lhuissier, P., Meyssonnier, J., Nguyen-Thi, H., Philip, A., Pernot, P., Salvo, L., Scheel, M. 2013. Synchrotron X-ray imaging for crystal growth studies. Comptes Rendus Physique 14(2-3): 208-220.

Despres, A., Pizzi, A. 2006. Colloidal aggregation of aminoplastic polycondensation resins: Urea–formaldehyde versus melamine–formaldehyde and melamine–urea–formaldehyde resins. Journal of Applied Polymer Science 100(2): 1406-1412.

Drnovšek, N., Kocen, R., Gantar, A., Drobnič-Košorok, M., Leonardi, A., Križaj, I., Rečnik, A., Novak, S. 2016. Size of silk fibroin β-sheet domains affected by Ca^{2+}. Journal of Materials Chemistry B 4(40): 6597-6608.

Ferg, E.E., Pizzi, A., Levendis, D.C. 1993. ^{13}C NMR analysis method for urea–formaldehyde resin strength and formaldehyde emission. Journal of Applied Polymer Science 50(5): 907-915.

Han, H., Lee, S., Yang, S., Choi, C., Kang, S. 2019. Evaluation of formaldehyde emission from wood-based panels using accelerated collection method. Journal of the Korean Wood Science and Technology 47(2): 129-144.

Hong, M.K., Lubis, M.A.R., Park, B.D. 2017. Effect of panel density and resin content on properties of medium density fiberboard. Journal of the Korean Wood Science and Technology 45(4): 444-455.

Jeong, B., Park, B.D. 2019. Performance of urea-formaldehyde resins synthesized at two different low molar ratios with different numbers of urea addition. Journal of the Korean Wood Science and Technology 47(2): 221-228.

Jeong, B., Park, B.D., Causin, V. 2020. Effects of storage time on molecular weights and properties of melamine-urea-formaldehyde resins. Journal of the Korean Wood Science and Technology 48(3): 291-302.

Keith Dunker, A., John, W.E., Rammon, R., Farmer, B., Johns, S.J. 1986. Slightly bizarre protein chemistry: Urea-formaldehyde resin from a biochemical perspective. The Journal of Adhesion 19(2): 153-176.

Kim, J.K., Lee, C., Lim, S.W., Adhikari, A., Andring, J.T., McKenna, R., Ghim, C.M., Kim, C.U. 2020. Elucidating the role of metal ions in carbonic anhydrase catalysis. Nature Communications 11(1): 4557.

Kim, M., Park, B.D. 2021a. A method of measuring wood failure percentage of wood specimens bonded with melamine-urea-formaldehyde resins using image analysis. Journal of the Korean Wood Science and Technology 49(3): 274-282.

Kim, M., Park, B.D. 2021b. Effects of synthesis method, melamine content and GPC parameter on the molecular weight of melamine-urea-formaldehyde resins. Journal of the Korean Wood Science and Technology 49(1): 1-13.

Kuei, B., Aplan, M.P., Litofsky, J.H., Gomez, E.D. 2020. New opportunities in transmission electron microscopy of polymers. Materials Science and Engineering: R: Reports 139: 100516.

Levendis, D., Pizzi, A., Ferg, E. 1992. The correlation of strength and formaldehyde emission with the crystalline/amorphous structure of UF resins. Holzforschung 46(3): 263-269.

Li, J., Zhang, Y. 2021. Morphology and crystallinity of urea-formaldehyde resin adhesives with different molar ratios. Polymers 13(5): 673.

Libera, M.R., Egerton, R.F. 2010. Advances in the transmission electron microscopy of polymers. Polymer Reviews 50(3): 321-339.

Lin, F., Liu, Y., Yu, X., Cheng, L., Singer, A., Shpyrko, O.G., Xin, H.L., Tamura, N., Tian, C., Weng, T.C., Yang, X.Q., Meng, Y.S., Nordlund, D., Yang, W., Doeff, M.M. 2017. Synchrotron X-ray analytical techniques for studying materials electrochemistry in rechargeable batteries. Chemical Reviews 117(21):

13123-13186.

Liu, M., Thirumalai, R.V.K.G., Wu, Y., Wan, H. 2017. Characterization of the crystalline regions of cured urea formaldehyde resin. RSC Advances 7(78): 49536-49541.

Lubis, M.A.R., Jeong, B., Park, B.D., Lee, S.M., Kang, E.C. 2019a. Effect of synthesis method and melamine content of melamine-urea-formaldehyde resins on bond-line features in plywood. Journal of the Korean Wood Science and Technology 47(5): 579-586.

Lubis, M.A.R., Park, B.D. 2020. Influence of initial molar ratios on the performance of low molar ratio urea-formaldehyde resin adhesives. Journal of the Korean Wood Science and Technology 48(2): 136-153.

Lubis, M.A.R., Park, B.D., Lee, S.M. 2019b. Performance of hybrid adhesives of blocked-pMDI/melamine-urea-formaldehyde resins for the surface lamination on plywood. Journal of the Korean Wood Science and Technology 47(2): 200-209.

Myers, G.E. 1984. How mole ratio of UF resin affects formaldehyde emission and other properties: A literature critique. Forest Products Journal 34(5): 35-41.

Nuryawan, A., Singh, A.P., Zanetti, M., Park, B.D., Causin, V. 2017. Insights into the development of crystallinity in liquid urea-formaldehyde resins. International Journal of Adhesion and Adhesives 72: 62-69.

Park, B.D., Causin, V. 2013. Crystallinity and domain size of cured urea–formaldehyde resin adhesives with different formaldehyde/urea mole ratios. European Polymer Journal 49(2): 532-537.

Park, B.D., Jeong, H.W. 2011. Hydrolytic stability and crystallinity of cured urea–formaldehyde resin adhesives with different formaldehyde/urea mole ratios. International Journal of Adhesion and Adhesives 31(6): 524-529.

Park, B.D., Jeong, H.W., Lee, S.M. 2011. Morphology and chemical elements detection of cured urea–formaldehyde resins. Journal of Applied Polymer Science 120(3): 1475-1482.

Park, S., Park, B.D. 2021. Crystallinity of low molar ratio urea-formaldehyde resins modified with cellulose nanomaterials. Journal of the Korean Wood Science and Technology 49(2): 169-180.

Pizzi, A., Lipschitz, L., Valenzuela, J. 1994. Theory and practice of the preparation of low formaldehyde emission UF adhesives. Holzforschung 48(3): 254-261.

Pratt, T.J., Johns, W.E., Rammon, R.M., Plagemann, W.L. 1985. A novel concept on the structure of cured urea-formaldehyde resin. The Journal of Adhesion 17(4): 275-295.

Schuett, T., Geitner, R., Zechel, S., Schubert, U.S. 2021. Dialysis diffusion kinetics in polymer purification. Macromolecules 54(20): 9410-9417.

Sedigh Rahimabadi, P., Khodaei, M., Koswattage, K.R. 2020. Review on applications of synchrotron-based X-ray techniques in materials characterization. X-Ray Spectrometry 49(3): 348-373.

Singh, A.P., Causin, V., Nuryawan, A., Park, B.D. 2014. Morphological, chemical and crystalline features of urea–formaldehyde resin cured in contact with wood. European Polymer Journal 56: 185-193.

Singh, A.P., Nuryawan, A., Park, B.D., Lee, K.H. 2015. Urea-formaldehyde resin penetration into *Pinus radiata* tracheid walls assessed by TEM-EDXS. Holzforschung 69(3): 303-306.

Steinhof, O., Kibrik, É.J., Scherr, G., Hasse, H. 2014. Quantitative and qualitative ^{1}H, ^{13}C, and ^{15}N NMR spectroscopic investigation of the urea–formaldehyde resin synthesis. Magnetic Resonance in Chemistry 52(4): 138-162.

Stuligross, J., Koutsky, J.A. 1985. A morphological study of urea-formaldehyde resins. The Journal of Adhesion 18(4): 281-299.

Tosaka, M., Danev, R., Nagayama, K. 2005. Application

of phase contrast transmission microscopic methods to polymer materials. Macromolecules 38(19): 7884-7886.

Wang, H., Cao, M., Li, T., Yang, L., Duan, Z., Zhou, X., Du, G. 2018. Characterization of the low molar ratio urea–formaldehyde resin with 13C NMR and ESI–MS: Negative effects of the post-added urea on the urea–formaldehyde polymers. Polymers 10(6): 602.

Wibowo, E.S., Lubis, M.A.R., Park, B.D. 2021. Simultaneous improvement of formaldehyde emission and adhesion of medium-density fiberboard bonded with low-molar ratio urea-formaldehyde resins modified with nanoclay. Journal of the Korean Wood Science and Technology 49(5): 453-461.

Wibowo, E.S., Lubis, M.A.R., Park, B.D., Kim, J.S., Causin, V. 2020a. Converting crystalline thermosetting urea–formaldehyde resins to amorphous polymer using modified nanoclay. Journal of Industrial and Engineering Chemistry 87: 78-89.

Wibowo, E.S., Park, B.D. 2020. Determination of crystallinity of thermosetting urea-formaldehyde resins using deconvolution method. Macromolecular Research 28(6): 615-624.

Wibowo, E.S., Park, B.D. 2021. Crystalline lamellar structure of thermosetting urea–formaldehyde resins at a low molar ratio. Macromolecules 54(5): 2366-2375.

Wibowo, E.S., Park, B.D. 2022. Two-dimensional nuclear magnetic resonance analysis of hydrogen-bond formation in thermosetting crystalline urea–formaldehyde resins at a low molar ratio. ACS Applied Polymer Materials 4(2): 1084-1094.

Wibowo, E.S., Park, B.D., Causin, V. 2020b. Hydrogen-bond-induced crystallization in low-molar-ratio urea –formaldehyde resins during synthesis. Industrial & Engineering Chemistry Research 59(29): 13095-13104.

Wibowo, E.S., Park, B.D., Causin, V. 2022. Recent advances in urea–formaldehyde resins: Converting crystalline thermosetting polymers back to amorphous ones. Polymer Reviews 62(4): 722-756.

Widjonarko, N.E. 2016. Introduction to advanced X-ray diffraction techniques for polymeric thin films. Coatings 6(4): 54.